NANO · MICRO small
www.small-journal.com

Eliminating Trap-States and Functionalizing Vacancies in 2D Semiconductors by Electrochemistry

Jianjian Shi, Xunhua Zhao, Zhiguo Wang, and Yuanyue Liu**

One major challenge that limits the applications of 2D semiconductors is the detrimental electronic trap states caused by vacancies. Here using grand-canonical density functional theory calculations, a novel approach is demonstrated that uses aqueous electrochemistry to eliminate the trap states of the vacancies in 2D transition metal dichalcogenides while leaving the perfect part of the material intact. The success of this electrochemical approach is based on the selectivity control by the electrode potential and the isovalence between oxygen and chalcogen. Motivated by these results, electrochemical conditions are further identified to functionalize the vacancies by incorporating various single metal atoms, which can bring in magnetism, tune carrier concentration/polarity, and/or activate single-atom catalysis, enabling a wide range of potential applications. These approaches may be generalized to other 2D materials. The results open up a new avenue for improving the properties and extending the applications of 2D materials.

2D transition metal dichalcogenides (MX_2, where M represents a metal element and X denotes a chalcogen) are one of the most common types of 2D materials and have shown great potential in electronic and optoelectronic applications.[1–5] However, one major challenge that limits their further developments is the detrimental electronic states induced by vacancies.[6–8] The vacancies create electronic states deep inside the bandgap that can trap electrons/holes,[6,7,9,10] scattering/recombining the charge carriers and thus decreasing their mobility and quantum efficiency. On the other hand, these vacancies may serve as potential sites for incorporating new elements, i.e., forming substitutional defects that may bring in new properties and functions. For example, Nb/Re substituting W in WSe_2 can induce p/n-type doping with long-term stability[11] compared with doping by molecule adsorption on the surface. Moreover, the substitutional metal atoms can activate the basal plane of MX2 by acting as single-atom catalysts for a variety of reactions.[12–15] Furthermore, incorporation of magnetic metal elements (e.g., Ni, Co) can introduce magnetism into nonmagnetic MX_2, which may be useful for spintronics.

To eliminate the trap states induced by vacancies, various approaches have been explored such as postannealing in chalcogen atmosphere[16] and treatments with molecular healing agents[17–19] or laser.[20] Here we demonstrate a facile approach that uses water to electrochemically eliminate the trap states of the anion vacancies (V_X, the most common defects in MX_2). We show that under proper potential, the O from water can be adsorbed into V_X, while formation of other adsorbates and reactions with the perfect part of the material are thermodynamically unfavorable. Since O is isovalent to X, the O adsorption into V_X thus eliminates the trap states (as demonstrated in refs. [9,20]). Therefore, the V_X is electronically passivated without contaminating the perfect part. Motivated by this success, we further study the electrochemical conditions to incorporate other single foreign atom into the vacancy, which can enable new functions.

A notable feature of electrochemical processes is that the reactions involve electrons/holes whose energetics can be tuned by the applied potential, which offers facile control over the reactions. This feature can be utilized to selectively passivate and/or functionalize the vacancies in 2D materials. **Figure 1** demonstrates the feasibility of using OH^- in aqueous solution to passivate V_X while leaving other parts intact. The calculations are performed using the grand-canonical density functional theory (DFT) method[21,22] as implemented in JDFTx code,[23] which captures the constant-potential effects and thus provides a better description of the electrochemical reactions than the conventional charge neutral DFT method. More computational details can be found in the Experimental Section. WSe_2, a common 2D semiconductor, is used as an example here. The OH^- can react with a site (denoted as *) and a hole (h) electrochemically through

$$OH^-(aq) + * + h \rightarrow *OH \quad (1)$$

forming an adsorbed OH. We find that this step is downhill in free energy (G) for * = V_{Se}, with a $\Delta G = -0.40$ eV at $U = 0$ V versus RHE (reversible hydrogen electrode) and $\Delta G = -2.75$ eV at $U = 1.23$ V versus RHE, suggesting that it is thermodynamically favorable for the V_{Se} to adsorb OH^- from solution coupled with charge transfer. We choose 0 and 1.23 V as potential limits

Dr. J. Shi, Dr. X. Zhao, Prof. Y. Liu
Texas Materials Institute and Department of Mechanical Engineering
The University of Texas at Austin
Austin, TX 78712, USA
E-mail: yuanyue.liu@austin.utexas.edu
Dr. J. Shi, Prof. Z. Wang
School of Information and Software Engineering
University of Electronic Science and Technology of China
Chengdu 610054, China
E-mail: zgwang@uestc.edu.cn
The ORCID identification number(s) for the author(s) of this article can be found under https://doi.org/10.1002/smll.201901899.

DOI: 10.1002/smll.201901899

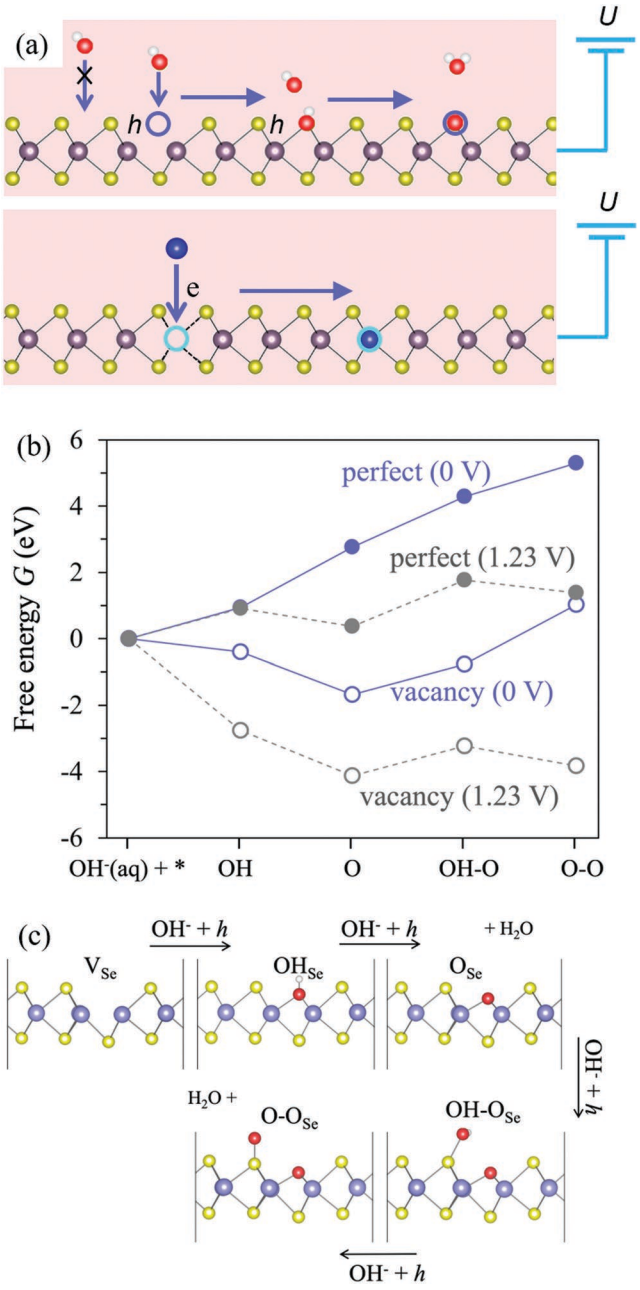

Figure 1. a) Schematic of using aqueous ions (OH^- or metal cations) to electrochemically passivate chalcogen vacancy (upper panel) or incorporate foreign metal element (lower panel). Since O is isovalent to X, the O adsorption into V_X thus eliminates the trap states (as demonstrated in refs. [9,20]). b) Free energy evolution of WSe_2 reacting with OH^- in water at pH = 13. Reactions on perfect site are indicated by filled circles, and those at V_{Se} are shown by hollow circles. Blue: 0 V versus RHE; gray: 1.23 V versus RHE. The free energy of OH^-(aq) + * system is set to be zero. c) The corresponding structures' evolution. Note that OOH_{Se} is unstable and will transform to $O{-}OH_{Se}$ during structure relaxation.

because a U lower/higher than 0/1.23 would result in splitting of bulk water through hydrogen evolution reaction (HER)/oxygen evolution reaction (OER); pH is set to be 13 in these calculations as a high concentration of OH^- can facilitate the reaction kinetically. A higher potential gives a stronger adsorption and lower formation free energy (G_f) of *OH because the hole energy is higher. The *OH may further react with OH^- and h through

$$*OH + OH^-(aq) + * + h \rightarrow *O + H_2O \quad (2)$$

Our calculations show that this step is also downhill at both $U = 0$ and 1.23 V for * = V_{Se}, resulting in the passivation of V_{Se} (the O in V_{Se} site is thereafter denoted as O_{Se}). It is possible that *O may further react with OH^- and h to form *OOH, similar to the step in the oxygen evolution reaction under alkaline conditions; however, we find that the *OOH at Se vacancy is unstable and will break to *O (at vacancy) and *OH (on the Se site near vacancy) during structural relaxation (see Figure 1), with an increase in free energy by 0.90 eV, suggesting that the O_{Se} is resistant to OH^- + h. It is also possible that V_{Se} adsorbs H through $H_2O + * + e \rightarrow *H_{Se} + OH^-$(aq), impeding the formation of O_{Se}; however, our calculations show that the G_f (H_{Se}) is 0.05 eV at $U = 0$ and 0.55 eV at $U = 1.23$ V, and thus the H_{Se} is thermodynamically unfavorable to form especially at high U (note that 0.05 eV ($\approx 2k_BT$) may be not sufficient to prevent the formation of Hs_e at room temperature, thus a higher U is recommended to avoid its formation). We have also calculated the G_f for *OO at V_{Se}, and find that it is larger than G_f (O_{Se}) by > 1 eV even at $U = 1.23$ versus RHE, indicating it is highly unfavorable to form. These results suggest that the passivation of V_{Se} by O is thermodynamically preferred compared with other adsorbates.

For * = Se in the perfect part of WSe_2, we have also considered various potential adsorbates, including *OH, *O, *OOH, *OO, and *H, to evaluate the possibility of surface contamination. The one with lowest G_f is either *OH or *O depending on the U (Figure 1), while both have a $G_f > 0$ through the 0–1.23 V, indicating that they are unlikely to form on pristine surface.

These results suggest general criteria of identifying the proper electrochemical conditions for vacancy passivation without damaging the perfect part of the material: the pathway to O_X should be downhill in free energy, while other potential adsorbates are thermodynamically unfavorable at the vacancy and on the pristine surface. Based on these criteria, any U between 0 and 1.23 V should work for WSe_2, although a high/low U may increase the possibility of surface contamination/H adsorption to V_{Se}. We have also studied other MX_2, including WS_2, $MoSe_2$, MoS_2 and $MoTe_2$ by calculating the critical potential (U_c) that leads to $G_f = 0$ for various potential adsorbates on different sites. The key results are shown in **Figure 2**. For all the materials, we find that the U should be < $U_c(O_{pft})$ (O_{pft} represents the configuration of O adsorbed perfect surface) to avoid surface contamination. Since the $U_c(O_X)$ is always < $U_c(OH_X)$, a $U > U_c(OH_X)$ leads to a downhill reaction to O_X. To avoid undesired H adsorption, the U should be larger than $U_c(H_{Se})$ since this reaction involves electron in the reactants. Taking these into account as well as the potential limits to avoid bulk water splitting, the working U range is marked in Figure 2 by the green arrows.

These results encourage us to explore the electrochemical conditions for incorporating other elements, such as metal

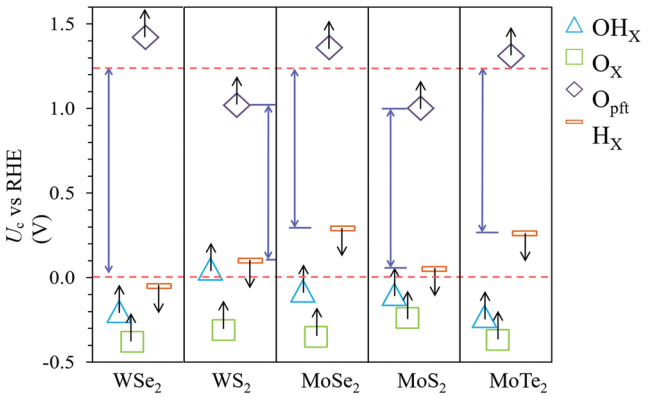

Figure 2. Critical potential (U_c) at which formation free energy (G_f) of adsorbate becomes zero. The single-headed arrows point to the potentials that make $G_f < 0$ for $*OH_X$ and $*O_X$, while $G_f > 0$ for $*OH_{pft}$ (pft stands for "perfect") and $*H_X$. The blue double-headed arrows mark the region where the O passivation of V_X is thermodynamically favorable without undesired side reactions. All the systems shown here are in aqueous solution with pH = 13.

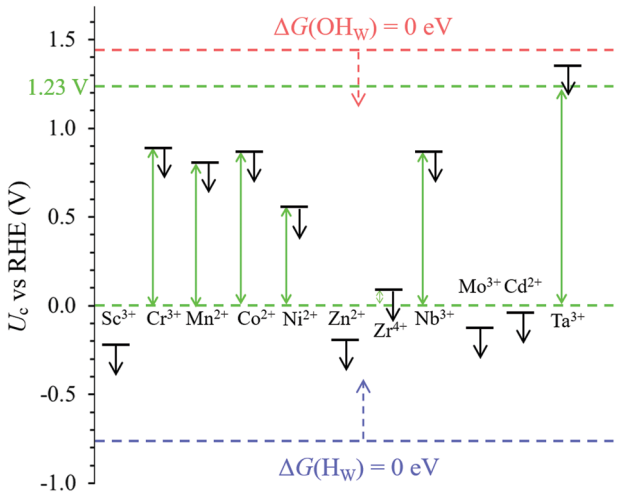

Figure 3. Critical potential (U_c) at which formation free energy (G_f) of adsorbate on V_W becomes zero. The single-headed arrows point to the potentials that make $G_f < 0$ for metal atoms, while $G_f > 0$ for *OH and *H. Green double-headed arrows mark the region where the incorporation of metal elements into V_W is thermodynamically favorable without undesired side reactions. All the systems shown here are in aqueous solution with 1 mol L^{-1} metal ions.

atoms. The metal atoms may be incorporated into vacancies through

$$M^{n+}(aq) + ne + * \rightarrow *M \quad (3)$$

Its feasibility can be evaluated using the formation free energy of the *M with respect to the reactants. A challenge for the computation is that the free energy of M^{n+}(aq) is difficult to calculate directly as it is hard to model a solvated ion accurately. Here, we utilize the experimental data of the standard electrode potential (U_0), which is the potential required to achieve the thermodynamic equilibrium

$$M^{n+}(aq) + ne \leftrightarrow M(bulk) \quad (4)$$

where M^{n+}(aq) is at the concentration of 1 mol L^{-1}. The U_0 is usually referred to the SHE (standard hydrogen electrode) that has the electron absolute energy of –4.44 eV, therefore, the electron energy at U_0 is $-4.44 - |e|U_0$. The energy of bulk M can be easily calculated using DFT, thus the free energy of M^{n+} can be obtained as

$$G(M^{n+}(aq)) = G(M(bulk)) - n(\mu_{SHE} - |e|U_0) \quad (5)$$

After getting the $G(M^{n+}(aq))$, the $G_f(*M)$ at different potentials and 1 mol L^{-1} M^{n+}(aq) can be obtained. Here we consider various metal ions that have fixed valence state through 0–1.23 V window. The U_c for making $G_f(*M) = 0$ eV at V_W of WSe_2 is shown in **Figure 3**. We find that the U_c for many metal elements falls within 0–1.23 V, and defines the upper limit of the working potential (i.e., only the lower potential can drive the reaction (3)). For Sc, Zn, Mo, and Cd, the U_c is < 0 V, suggesting that the HER of bulk water should also take place when these elements are incorporated. While for Ta, the U_c is higher than 1.23 V, thus the formation of Ta_W should be thermodynamically favorable through the 0–1.23 V window. We have also tested other potential adsorbates on V_W, including *H and OH*. Their adsorptions are thermodynamically unfavorable as their U_c falls outside of 0–1.23 V (U_c = –0.77 V for *H and 1.47 V for *OH). The adsorption of metal atoms on perfect sits is also unfavorable because the U_c is much lower than 0 V. Taking all these factors into account, the working potential range is marked in Figure 3 using green arrows.

It is also interesting to explore the applicability of the electrochemical method to incorporate metal atoms into Se vacancies. However, we find that the U_c is well below 0 V for all the metal elements considered here, therefore, they are unlikely to be adsorbed. The difference in metal incorporation between V_{Se} and V_W can be explained by the stronger bonding of metal with chalcogen than the bonding between different metal atoms.

In summary, we demonstrate a facile approach that uses water to electrochemically eliminate the trap states of the vacancies at room temperature and identified the working potentials using first-principles calculations. Under proper potentials, the O from water can be adsorbed into V_X removing the electronic trap states due to the isovalence between O and X, while formation of other adsorbates and reactions with the perfect part of the material are thermodynamically unfavorable. In the same spirit, we studied also the electrochemical conditions to incorporate other single foreign atom into the vacancy, which can be used to improve and extend the function of 2D materials.

Experimental Section

To obtain the energetics for electrochemical reactions, we used constant-potential method[21,22] as implemented in JDFTx code.[23] We used Garrity–Bennett–Rabe–Vanderbilt (GBRV) ultrasoft pseudopotentials,[24] with an energy cutoff of 20 Hartree, and the charge-asymmetric

nonlocally-determined local-electric (CANDEL)[25] implicit solvation model. Using the $OH^-(aq) + h \rightarrow *OH$ as an example, here we show how to calculate the free energy change (ΔG) of the reaction. In this example,

$$\Delta G = G(*OH^{Q2}) - G(*^{Q1}) - G(OH^-)(aq) + (Q2 - Q1 + 1)\mu_e \quad (6)$$

where Q1 and Q2 are the net charges (obtained from JDFTx) on the solid before and after the adsorption. μ_e is the electron energy and can be calculated as

$$\mu_e = \mu_{SHE} - |e|U_{SHE} \quad (7)$$

where U_{SHE} is the applied voltage versus SHE, and $\mu_{SHE} = -4.66$ eV (μ_{SHE} in the JDFTx is different from the experimentally measured value)

$G(OH^-)$ is calculated by

$$G(OH^-) = G(H_2O) - G(H^+) = G(H_2O) - \left[1/2G(H_2(g)) - \mu_{SHE} - 0.059 \times pH\right] \quad (8)$$

$G(*OH^{Q2})$ and $G(*^{Q1})$ are calculated by summing the adsorbate vibration contribution to the free energy with the electronic energy (obtained from JDFTx), and the $G(H_2)$ is calculated by summing the vibration, translation, and rotation contributions (calculated using Gaussian software) at standard conditions with the electronic energy.

Similarly, we can obtain ΔG for other reactions. The formation free energy of an adsorbate is obtained by summing up ΔG for all the reactions along the pathway toward the formation of the adsorbate.

Acknowledgements

J.S. and X.Z. contributed equally to this work. Y.L. thanks Zhengzong Sun (Fudan U.) and Mengning Ding (Nanjing U.) for valuable discussions. This work was partially supported by the Welch Foundation (Grant No. F-1959-20180324) and the National Science Foundation (Grant No. 1900039), and used the computational resources at (1) National Renewable Energy Lab (sponsored by the DOE's Office of EERE), (2) the Extreme Science and Engineering Discovery Environment (XSEDE) through allocation TG-CHE190065, (3) the Center for Nanoscale Materials (a DOE Office of Science user facility supported under Contract No. DE-AC02-06CH11357) at Argonne National Lab, and (4) the Center for Nanophase Materials Sciences (a DOE Office of Science user facility) at Oak Ridge National Lab.

Conflict of Interest

The authors declare no conflict of interest.

Keywords

defects, electrochemistry, grand-canonical DFT calculations, 2D semiconductors

Received: April 15, 2019
Revised: August 24, 2019
Published online: October 22, 2019

[1] X. Duan, C. Wang, A. Pan, R. Yu, X. Duan, *Chem. Soc. Rev.* **2015**, *44*, 8859.
[2] N. Briggs, S. Subramanian, Z. Lin, X. Li, X. Zhang, K. Zhang, K. Xiao, D. Geohegan, R. Wallace, L.-Q. Chen, M. Terrones, A. Ebrahimi, S. Das, J. Redwing, C. Hinkle, K. Momeni, A. van Duin, V. Crespi, S. Kar, J. A. Robinson, *2D Mater.* **2019**, *6*, 022001.
[3] Y. Sun, K. Fujisawa, Z. Lin, Y. Lei, J. S. Mondschein, M. Terrones, R. E. Schaak, *J. Am. Chem. Soc.* **2017**, *139*, 11096.
[4] A. D. Oyedele, S. Yang, L. Liang, A. A. Puretzky, K. Wang, J. Zhang, P. Yu, P. R. Pudasaini, A. W. Ghosh, Z. Liu, C. M. Rouleau, B. G. Sumpter, M. F. Chisholm, W. Zhou, P. D. Rack, D. B. Geohegan, K. Xiao, *J. Am. Chem. Soc.* **2017**, *139*, 14090.
[5] J. Wang, H. Fang, X. Wang, X. Chen, W. Lu, W. Hu, *Small* **2017**, *13*, 1700894.
[6] H.-P. Komsa, A. V. Krasheninnikov, *Phys. Rev. B* **2015**, *91*, 125304.
[7] J. Hong, Z. Hu, M. Probert, K. Li, D. Lv, X. Yang, L. Gu, N. Mao, Q. Feng, L. Xie, J. Zhang, D. Wu, Z. Zhang, C. Jin, W. Ji, X. Zhang, J. Yuan, Z. Zhang, *Nat. Commun.* **2015**, *6*, 6293.
[8] C. Zhang, C. Wang, F. Yang, J.-K. Huang, L.-J. Li, W. Yao, W. Ji, C.-K. Shih, *ACS Nano* **2019**, *13*, 2520.
[9] Y. Liu, P. Stradins, S.-H. Wei, *Angew. Chem., Int. Ed.* **2016**, *55*, 965.
[10] L. Zhong, R. C. Bruno, K. Ethan, L. Ruitao, R. Rahul, T. Humberto, A. P. Marcos, T. Mauricio, *2D Mater.* **2016**, *3*, 022002.
[11] R. Mukherjee, H. J. Chuang, M. R. Koehler, N. Combs, A. Patchen, Z. X. Zhou, D. Mandrus, *Phys. Rev. Appl.* **2017**, *7*, 034011.
[12] H. Li, L. Wang, Y. Dai, Z. Pu, Z. Lao, Y. Chen, M. Wang, X. Zheng, J. Zhu, W. Zhang, R. Si, C. Ma, J. Zeng, *Nat. Nanotechnol.* **2018**, *13*, 411.
[13] J. Deng, H. Li, J. Xiao, Y. Tu, D. Deng, H. Yang, H. Tian, J. Li, P. Ren, X. Bao, *Energy Environ. Sci.* **2015**, *8*, 1594.
[14] Y. Chen, S. Ji, C. Chen, Q. Peng, D. Wang, Y. Li, *Joule* **2018**, *2*, 1242.
[15] G. Liu, A. W. Robertson, M. M.-J. Li, W. C. H. Kuo, M. T. Darby, M. H. Muhieddine, Y.-C. Lin, K. Suenaga, M. Stamatakis, J. H. Warner, S. C. E. Tsang, *Nat. Chem.* **2017**, *9*, 810.
[16] J. Shimizu, T. Ohashi, K. Matsuura, I. Muneta, K. Kakushima, K. Tsutsui, H. Wakabayashi, *Jpn. J. Appl. Phys.* **2017**, *56*, 04CP06.
[17] A. Förster, S. Gemming, G. Seifert, D. Tománek, *ACS Nano* **2017**, *11*, 9989.
[18] M. Amani, D.-H. Lien, D. Kiriya, J. Xiao, A. Azcatl, J. Noh, S. R. Madhvapathy, R. Addou, S. Kc, M. Dubey, K. Cho, R. M. Wallace, S.-C. Lee, J.-H. He, J. W. Ager, X. Zhang, E. Yablonovitch, A. Javey, *Science* **2015**, *350*, 1065.
[19] M. Amani, P. Taheri, R. Addou, G. H. Ahn, D. Kiriya, D.-H. Lien, J. W. Ager, R. M. Wallace, A. Javey, *Nano Lett.* **2016**, *16*, 2786.
[20] J. Lu, A. Carvalho, X. K. Chan, H. Liu, B. Liu, E. S. Tok, K. P. Loh, A. H. Castro Neto, C. H. Sow, *Nano Lett.* **2015**, *15*, 3524.
[21] R. Sundararaman, W. A. Goddard III, T. A. Arias, *J. Chem. Phys.* **2017**, *146*, 114104.
[22] D. Kim, J. Shi, Y. Liu, *J. Am. Chem. Soc.* **2018**, *140*, 9127.
[23] R. Sundararaman, K. Letchworth-Weaver, K. A. Schwarz, D. Gunceler, Y. Ozhabes, T. A. Arias, *SoftwareX* **2017**, *6*, 278.
[24] K. F. Garrity, J. W. Bennett, K. M. Rabe, D. Vanderbilt, *Comput. Mater. Sci.* **2014**, *81*, 446.
[25] R. Sundararaman, W. A. Goddard, *J. Chem. Phys.* **2015**, *142*, 064107.

